Application of Fast Perturbational Complexity Index to the Diagnosis and Prognosis for Disorders of Consciousness

Yong Wang, Zikang Niu, Xiaoyu Xia, Yang Bai, Zhenhu Liang, Jianghong He, and Xiaoli Li

***Abstract*— *Objective:* Diagnosis and prognosis of patients with disorders of consciousness (DOC) is a challenge for neuroscience and clinical practice. Transcranial magnetic stimulation combined with electroencephalography (TMS-EEG) is an effective tool to measure the level of consciousness. However, a scientific and accurate method to quantify TMS-evoked activity is still lacking. This study applied fast perturbational complexity index (PCIst) to the diagnosis and prognosis of DOC patients. *Methods:* TMS-EEG data of 30 normal healthy participants (NOR) and 181 DOC patients were collected. The PCIst was used to assess the time-space complexity of TMS-evoked potentials (TEP). We selected parameters of PCIst in terms of data length, data delay, sampling rate and frequency band. In addition, we collected Coma Recovery Scale–Revised (CRS-R) values for 114 DOC patients after one year. Finally, we trained the classification and regression model. *Results:* 1) PCIst shows the differences among NOR, minimally consciousness state (MCS) and unresponsive wakefulness syndrome (UWS) and has low computational cost. 2) Optimal parameters of data length and delay after TMS are 300 ms and 101–300 ms. Significant differences of PCIst at 5–8 Hz and 9–12 Hz bands are found among NOR, MCS and UWS groups. PCIst still works when TEP is down-sampled to 250 Hz. 3) PCIst at 9–12 Hz shows the highest performance in diagnosis and prognosis of DOC. *Conclusions:* This study confirms that PCIst can quantify the level of consciousness. PCIst is a potential measure for the diagnosis and prognosis of DOC patients.**

***Index Terms*— TMS-EEG, PCIst, DOC, diagnosis, prognosis.**

I. Introduction

SEVERE brain injury leads to disorders of consciousness (DOC), and DOC patients show none or only some behavioral signs of consciousness [1]. DOC includes unresponsive wakefulness syndrome (UWS), formerly called vegetative state, and minimally consciousness state (MCS) [2]–[4]. Some patients fully recover consciousness and even return to normal life after long-term treatment and care from doctors and family members; some patients remain in unconscious state for long time, leading to extended grief and treatment costs. A reliable clinical diagnosis contributes to medical decisions for DOC. It is very important to identify signs of consciousness recovery [4]. The Coma Recovery Scale–Revised (CRS-R) is the gold standard for clinical assessment of consciousness level [5]. It measures patients' consciousness level by behavioral responses to external stimulation. However, limited by the operator's proficiency and patient's cooperation, a study found that CRS-R had a 40% misdiagnosis rate in the clinical diagnosis of DOC [6]. In recent years, electroencephalography (EEG), as a convenient brain activity monitoring tool, has been used in the study of brain functional diseases, such as major depressive disorder [7], epilepsy [8], [9] and DOC [10]–[15]. Lehembre et al reviewed EEG research in DOC and found that quantitative EEG features can distinguish UWS and MCS at the group level [16]. For future research, it has been suggested that large amounts of data can describe EEG pattern characteristics of different consciousness states in detail. Sitt et al reported differences of different consciousness states in terms of EEG power spectra, complexity and functional connectivity. They trained machine learning models for diagnosing patients from different institutions [14]. However, the above EEG studies cannot quantify the level of consciousness of patients at the individual level, nor did they study the predictive ability of EEG on patients' recovery outcome.

Transcranial magnetic stimulation combined with electroencephalography (TMS-EEG) is an effective way to measure cortical activity. TMS-EEG was used to further study cortical characteristics by TMS-evoked potential (TEP) [18], TMS-evoked oscillations [19] and TMS-evoked connectiv-

Manuscript received June 20, 2021; revised November 27, 2021, January 9, 2022, and February 11, 2022; accepted February 23, 2022. Date of publication February 25, 2022; date of current version March 11, 2022. This work was supported in part by the Scientific and Technological Innovation 2030 under Grant 2021ZD0204300; in part by the National Natural Science Foundation of China under Grant 61827811, Grant 81771128, and Grant 62073280; and in part by the Key Research and Development Program of Guangdong Province, China, under Grant 2018B030339001. *(Yong Wang and Zikang Niu contributed equally to this work.) (Corresponding authors: Jianghong He; Xiaoli Li.)*

This work involved human subjects or animals in its research. Approval of all ethical and experimental procedures and protocols was granted by the Seventh Medical Center of the General Hospital, Chinese PLA.

Yong Wang, Zhenhu Liang, and Xiaoli Li are with the Department of Electrical Engineering and the Key Laboratory of Intelligent Rehabilitation and Neuromodulation of Hebei Province, Yanshan University, Qinhuangdao, Hebei 066004, China (e-mail: wangyong0303@stumail.ysu.edu.cn; zhl@ysu.edu.cn; xiaoli@bnu.edu.cn).

Zikang Niu is with the State Key Laboratory of Cognitive Neuroscience and Learning and the IDG/McGovern Institute for Brain Research, Beijing Normal University, Beijing 100875, China (e-mail: 201831061058@bun.edu.cn).

Xiaoyu Xia is with the Senior Department of Neurosurgery, The First Medical Center of PLA General Hospital, Beijing 100700, China (e-mail: jiaxy02@163.com).

Yang Bai is with the Department of Basic Medical Science, School of Medicine, Hangzhou Normal University, Hangzhou, Zhejiang 311121, China (e-mail: baiyang1126@gmail.com).

Jianghong He is with the Department of Neurosurgery, Beijing Tiantan Hospital, Capital Medical University, Beijing 100070, China (e-mail: he_jianghong@sina.cn).

Digital Object Identifier 10.1109/TNSRE.2022.3154772

ity [17], [20]. TEP is a complex waveform composed of excitatory and inhibitory potentials of cortical synaptic cells stimulated by TMS, which has high repeatability [21]. The TEP components related to primary motor area include N15, P30, N45, P55, N100, P180 and N280 [22] and the TEP components evoked by dorsolateral prefrontal cortex include P30, N40, P60, N100 and P185 [23]. It has been reported that early TEP components are related to the cortical excitability of stimulation sites, and N100 represents the cortical inhibition induced by GABAB [23]. TEP is very sensitive to the brain state. Subject showed simple and local TEP components localized at the stimulation site during general anesthesia and during slow wave sleep [24], [25]. TEP can characterize the dynamic changes of cortical activity. TEP was used to distinguish patients with different states of consciousness (MCS, UWS) [26], and TEP components improved during consciousness recovery [11]. In addition, TEP was used to study the effect of neural modulation on cortical activity. Pedro et al used TEP to study modulation effects of tDCS on cortical excitability [27]. Bai et al showed that rTMS and tDCS affect cortical excitability of patients with DOC by changes of TEP [28], [29]. The current topography and cortical source distribution of TEP can be used to study the connectivity between stimulation cortex and other cortices [11], [26]. Rosanova et al reported that UWS patients showed a small number of TMS-evoked sources around the stimulated site, while MCS patients showed complex TMS-evoked sources from the stimulated site to a large number of distant cortices [11]. Imaging studies confirmed the interactions between cortex and subcortical structures after TMS, and explained the neural structural basis of cortical connectivity [30].

TMS-evoked oscillations can explore the intrinsic characteristics of cortex in the frequency domain. Studies have found that TMS at different cortical sites can evoke oscillations in different frequency bands. For example, TMS can evoke 21-50 Hz frequency band oscillation in frontal cortex [19]. A study of schizophrenia found that gamma band activity at frontal lobe was abnormal in patients with first-episode and chronic schizophrenia. This study provided an electrophysiological basis for understanding the brain structural abnormalities in patients with schizophrenia [31], [32]. Longitudinal measurements of TMS-EEG found that alpha band oscillation was a potential biomarker for stroke patients' recovery, and it was helpful for configuring time scheme settings of neural modulation [33]. A study of Parkinson found that DBS could improve the beta band activity of primary motor cortex in patients, which was helpful for understanding the mechanism of DBS [34]. In general, TMS-EEG provides a powerful research tool to help understand the intrinsic mechanism of the healthy and diseased brain.

A reliable and accurate quantitative index of TMS-EEG based on scientific algorithm will promote its practical application. Adenauer et al proposed a quantitative index, called perturbational complexity index (PCI), which combined non-parametric bootstrap-based statistical procedure and Lempel-Ziv complexity to quantify the temporal and spatial complexity of TMS-evoked cortical excitatory activity [35]. PCI indirectly quantifies the effective connectivity between cortices by temporal and spatial significant activation of TEP. And the cortical effective connectivity contributes to consciousness. Unconscious states caused by different reasons (physiology, pharmacology and pathology) showed low PCI. PCI was positively correlated with the level of consciousness [26]. When PCI < 0.3, participants were in slow wave sleep, under anesthesia or in UWS. When PCI > 0.3, participants were awake or in MCS. Research on DOC showed that the increase of PCI was parallel to the improvement of consciousness level [28].

However, PCI has some shortcomings. First, PCI must determine the real activation cortical source based on statistical analysis. The cortical source location and nonparametric statistics increase the operational difficulty and the amount of computation; Second, Lempel-Ziv complexity needs to search number of special subsequences as well as the rate of their recurrence in TMS-EEG data, which further increases the computational cost. The large amount of computation limits its real-time application.

In view of this, Renzo et al proposed a PCIst algorithm [36], which can obtain significant spatial components of TMS-EEG by principal component analysis, and then obtain temporal complexity by recurrence quantification analysis (RQA). PCIst has broad applicability. PCIst is not only faster than Lempel-Ziv PCI, but also stable for TMS-EEG data with a small number of channels.

We collected TMS-EEG data from normal healthy participants and DOC patients and compared Lempel-Ziv PCI with fast PCI of TMS-EEG data in different consciousness states. Second, we investigated parameter selection for calculating PCIst, including data length, data delay, sampling rate and frequency band. Finally, we explored the diagnostic and prognostic applicability of PCIst in DOC patients.

II. Materials and Methods

A. Subjects

We collected TMS-EEG data from 30 normal healthy participants and 181 DOC patients. The study was approved by the ethics committee of the Seventh Medical Center of the General Hospital of the Chinese PLA (NO.2016-63). The date of approval: October 31, 2016. All participants (normal healthy adults) or their families (DOC patients) were informed of the details of the study and provided written consent. The age range of the 30 normal people was 33-64 years old and included 15 males and 15 females. None of the participants had a history of skull defect or epilepsy, and they recently did not take any sedatives. 181 patients with DOC, aged 20-60 years, included 120 males and 61 females. The patients' conditions were stable and their skulls were intact. The experiment was terminated if a patient had unexpected situations during data collection, including changes in condition, high muscle tension, and constant jaw clenching. The basic information of participants is shown in Table I.

B. CRS-R Data Acquisition

1) Baseline CRS-R: All DOC patients received CRS-R assessment in baseline level, performed by an experienced neurosurgeon. CRS-R is a stimulus-feedback assessment method, which includes five sub-items involving 23 behaviors Sub-items includes arousal, oral movement, movement, vision and

TABLE I
INFORMATION OF PARTICIPANTS

Group	Age (mean ± SD)	Sex (m + f)	Pathogeny			Course of disease(mo)	CRS-R (mean ± SD)
			Trauma	Hemorrhage	Hypoxia		
NOR	48.36±7.47	15+15	0	0	0	0	--
MCS	49.67±13.05	47+29	22	35	19	6.74±7.14	9.44±2.36
UWS	45.01±14.08	73+32	22	41	42	4.84±4.61	5.75±1.47

NOR: normal healthy adults, MCS: minimally consciousness state, UWS: unresponsive wakefulness syndrome, m: male, f: female, mo: month.

hearing. Among them, visual object tracking, auditory location and stimulus location are key behavioral characteristics for MCS. Each DOC patient received CSR-R assessment three times while awake, each time taking about 1 hour. At last, the highest score was taken as the CSR-R score of the patient.

2) CRS-R After One Year: We got outcome of 114 patients with DOC after one year. The neurosurgeon cooperated with the patient's family to assess the patient's CRS-R score through smartphone video. A study has reported the reliability of real-time video by smartphone for behavioral assessment of stroke patients [37]. 114 patients were divided into 2 groups, good and poor group. Patients in the poor group did not show any improvement of CRS-R score; Patients in the good group had behaviors related to consciousness and improvement of CRS-R scores.

C. TMS-EEG Data Acquisition

This study used a TMS-compatible BrainAmp amplifier (Brain Products, Germany) with a 64 TMS-compatible Ag/AgCl electrode cap (EASYCAP GmbH, Germany). The sampling rate was 2500 Hz. We used a Magstim R2 stimulator with a 70-mm air-cooled figure of eight coil (Magstim Company Limited, Whitland, UK). The cap was placed on the participants' heads, and the impedance was below 5 KΩ before recording data. The stimulation site was localized over the F3 electrode (dorsolateral prefrontal area) of the electrode cap. The coil was placed tangentially to the stimulation site at about 45° angle away from the midline with a posterior–anterior current flow in the underlying cortex. In order to avoid possible auditory responses and the bone-conducted sound caused by the TMS click, the participants wore earphone with a white noise masking sound, and a thin sponge was placed under the coil. TMS-EEG data included 200 single TMS pulses with time interval of 2.2s-2.5s. The TMS stimulation intensity was 90% of the resting motor threshold (RMT), and RMT was the minimum stimulation intensity to evoke 50μV peak-to-peak MEP amplitude at least 5 of 10 trials in the relaxed first dorsal interosseous muscle. A single TMS-EEG data acquisition session took 45-60 minutes All participants did not take sedative drugs during data acquisition.

D. TMS-EEG Data Preprocessing

In this study, we preprocessed the TMS-EEG data by the TMS-EEG signal analyzer software (TESA) [38] in MATLAB (R2020a, the Mathworks, USA). The processing steps are as follows: (1) Import the original data and configure the electrode positions. (2) Check the original data to find bad electrodes, and replace bad electrodes with the average value of the surrounding electrodes. (3) Epoch original data around the TMS pulse from −1000ms to 1000ms and baseline correct using data from −500ms to 0ms. Remove the TMS pulse artifact and high peaks related to TMS-evoked muscle activity around the TMS pulse from −10ms to 10ms and interpolate the missing data with a cubic function. (4) Inspect all epochs, delete epochs with poor quality (24.26±13.55, the radio between deleted epochs and retained epochs: 0.18±0.11) and down-sample data to 1000Hz. (5) Perform first ICA, extract top 15 components, and remove ones on TMS-evoked muscle, electrical, and movement artifacts (2.26±0.74). (6) Apply a Butterworth, zero-phase band-pass filter (1-40 Hz) to the data. (7) Perform second ICA, extract retained components (57.74±0.74) and remove ones reflecting eye blinks, eye movement, persistent muscle activity and electrode noise (27.03±7.49). (8) Re-reference data to a common average.

E. Source Localization

In this study, the source location of TMS-EEG was calculated by the Brainstorm software package, as follows: (1) Import anatomical structure data, including relationships of cortex, skull, scalp and electrode position; (2) Use OpenMEEG BEM, a forward modeling method, to calculate the head model; (3) Based on the head model, estimate the source current by minimum norm imaging; (4) Use nonparametric permutation t-test to compare the differences in source currents before and after stimulation, to find sources with significant changes after stimulation ($p < 0.01$ followed by post hoc FDR corrected t-test).

F. PCI-lz

PCI based on the Lempel-Ziv algorithm (PCI-lz) is proposed by Adenauer et al [35] and calculated as follows: (1) Calculate the primary electromagnetic sources of TMS-EEG by source location. (2) A non-parametric bootstrap-based statistical procedure to estimate the deterministic responses of TMS-evoked cortical activity. A binary spatiotemporal distribution of significant sources is calculated. (3) Apply the Lempel-Ziv measure to the binary matrix to evaluate the information content of TMS-evoked cortical activity. (4) Define the PCI-lz as the normalized Lempel-Ziv complexity of TMS-evoked cortical activation.

G. PCIst

PCIst is a quantitative index of TMS-EEG proposed by Renzo et al [36], which combines singular value

decomposition and recurrence analysis to quantify the spatiotemporal complexity of TEP. Research showed that PCIst can quantify the level of consciousness and is more practical than PCI based on the Lempel-Ziv algorithm, especially in terms of computational cost. The calculation process is as follows:

We calculate the average TEP of all trials, defined as $A(n, t)$, n is the number of channels, t is the number of time samples.

Firstly, singular value decomposition is used to decompose the signal.

$$Ax_i = \lambda_i x_i \tag{1}$$

Secondly, calculate the ratio of eigenvalues λ and the signal-to-noise ratio of eigenvector signal Ax, and select the principal component signals.

$$Ratio(i) = \frac{(\lambda_i)^2}{\sum(\lambda_i)^2}, \tag{2}$$

$$SNR_i = \sqrt{\frac{\frac{1}{Tafter}\sum_0^{Tafter}|Ax_i(t)|^2}{\frac{1}{Tbfore}\sum_{-Tbfore}^{0}|Ax_i(t)|^2}} \tag{3}$$

where we select the eigenvector signals whose sum of eigenvalue proportion is greater than 0.99 and each SNR is greater than 1.2.

Thirdly, recurrence quantification analysis is used to quantify the change of single principal component before and after TMS, and get matrix $D_{j,k}$(before) and $D_{j,k}$(after)

$$D_{j,k}(\text{before}) = \|Ax_i(j) - Ax_i(k)\|, \tag{4}$$

where $-Tbefore < j,\ k < 0$.

$$D_{j,k}(\text{after}) = \|Ax_i(j) - Ax_i(k)\|, \tag{5}$$

where $0 < j,\ k < Tafter$.

Fourthly, it uses the threshold to binarize the matrix $D_{j,k}$(before) and $D_{j,k}$(after) and gets transition matrix $\text{Tr}_{j,k}$(before) and $\text{Tr}_{j,k}$(after). The difference between the two matrices is calculated and normalized to obtain the spatiotemporal quantization value of a single principal component signal PST_{ii}.

$$PST_{ii} = \frac{sum\left(\text{Tr}_{j,k}(after)\right) - sum\left(\text{Tr}_{j,k}(before)\right)}{Tbefore * Tbefore}, \tag{6}$$

Fifthly, PCIst can be obtained by accumulating the quantized value of principal component signals.

We investigate the parameter selection for PCIst in terms of data length, data delay, sampling rate and frequency band. The baseline TEP is from −400 to −50ms. We use different parameters for PCIst: (1) Data length after TMS: from 100ms to 300ms with step size 100ms. (2) Data delay after TMS: 21-100ms, 101-200ms, or 201-300ms. (3) Sampling rate: 1000Hz, 500Hz and 250Hz. (4) Frequency band of TEP: delta: 1-4Hz, theta: 5-8Hz, alpha: 9-12Hz, beta: 13-20Hz and gamma: 21-45Hz.

H. Statistical Analysis

In all conditions, we perform the Kolmogorov-Smirnov test to evaluate the normal distribution of the data (all $p > 0.2$). One-way ANOVA is used to measure differences of PCIst and PCI-lz among three group. Two sample t-test is performed to measure difference between NOR and MCS, MCS and UWS. So do the computation time. Besides, difference of the computation time between PCIst and PCI-lz is also measured.

The differences of PCIst are measured by three-way repeated-measures ANOVA with *time* (*data length and delay*), *frequency band* and *group*; with *Sampling rate*, *frequency band* and *group*. Because short data length(100ms) with low sampling rate (500Hz, 250Hz) cannot get an accurate PCIst. A value $p < 0.05$ is the threshold for significance. Conditional on a significant F value, we perform post-hoc t-tests (FDR) based on Benjamini-Hochberg algorithm to explore the main effects and the interaction effects between the factors ($p < 0.025$). The degrees of freedom(df) and effect sizes of Cohen's d are calculated too.

1) Features Selection: Pearson correlation between quantitative indexes of TMS-EEG and CRS-R is calculated and a value $p<0.05$ is the threshold for significance. Arrange all indexes in descending order according to the correlation coefficient. The top three indexes are used to train the classification and regression models.

2) Models: We use support vector machine (SVM) with linear function kernels to train classification and regression models. We perform repeated k-folds cross-validate (5 folds, 20 repetitions). (1) The data are randomly divided into 5 copies. (2) One is used as validation data and the other four are for training the model. (3) Repeat step (2) 5 times with different copies as validation data each time. All samples are training data and validation data. (4) Repeat steps (1)-(3) 20 times and calculate the average performance index of the models.

3) Performances: Area under the carve (AUC) based on receiver operating characteristic (ROC) and accuracy (ACC) are used to assessed the performance of models. We calculate the sensitivity (SEN), the specificity (SPE), F1 score and accuracy (ACC), as follows:

$$SEN = \text{TP}/(\text{TP} + \text{FN}), \tag{7}$$

$$SPE = \text{TN}/(\text{FP} + \text{TN}), \tag{8}$$

$$ACC = (\text{TP} + \text{FP})/(\text{TP} + \text{FN}), \tag{9}$$

$$F1 = \frac{2 * (\text{TP}/(\text{TP} + \text{FP})) * (\text{TP}/(\text{TP} + \text{FN}))}{(\text{TP}/(\text{TP} + \text{FP})) + (\text{TP}/(\text{TP} + \text{FN}))} \tag{10}$$

where TP, TN, FP, and FN are the number of true positives, true negatives, false positives, and false negatives, respectively.

III. Results

A. Results of PCIst and PCI-lz

PCIst and PCI-lz show significant differences among different consciousness states ($F = 69.55$, $p < 0.001$, $df = 212$, Cohen's $d = 0.40$; $F = 77.11$, $p < 0.001$, $df = 212$, Cohen's $d = 0.42$). The computation time (Figure 1B) of PCIst is lower than that of PCI-lz ($p < 0.005$, $df = 424$, Cohen's $d = 0.99$). In addition, the computation time for the NOR group is higher than MCS ($p < 0.005$, $df = 106$, Cohen's $d = 0.57$).

B. Results of TMS-EEG

The results of TMS-EEG for NOR, MCS and UWS groups are shown in Figure 2. The TEP of NOR consists of a

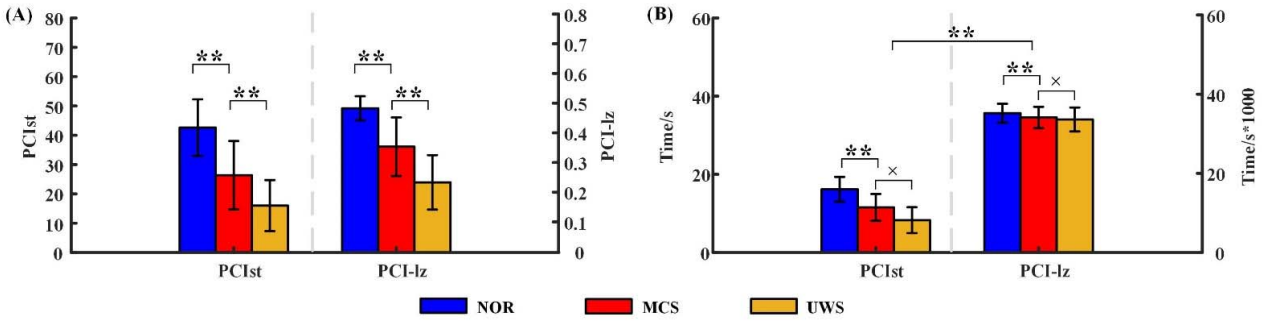

Fig. 1. Results of PCIst and PCI-lz among groups. (A) PCIst and PCI-lz values. (B) Computation time. NOR: normal healthy adults, MCS: minimally consciousness state, UWS: unresponsive wakefulness syndrome. Left ordinate of (A, B) is for PCIst, while right ordinate of (A, B) is for PCI-lz. Note: ×means p>0.05, *means p<0.05, **means p<0.005 followed by post hoc FDR corrected t-test. PCIst means fast PCI, PCI-lz means Lempel-Ziv PCI. The bars represent the mean and error bars represent the standard deviation.

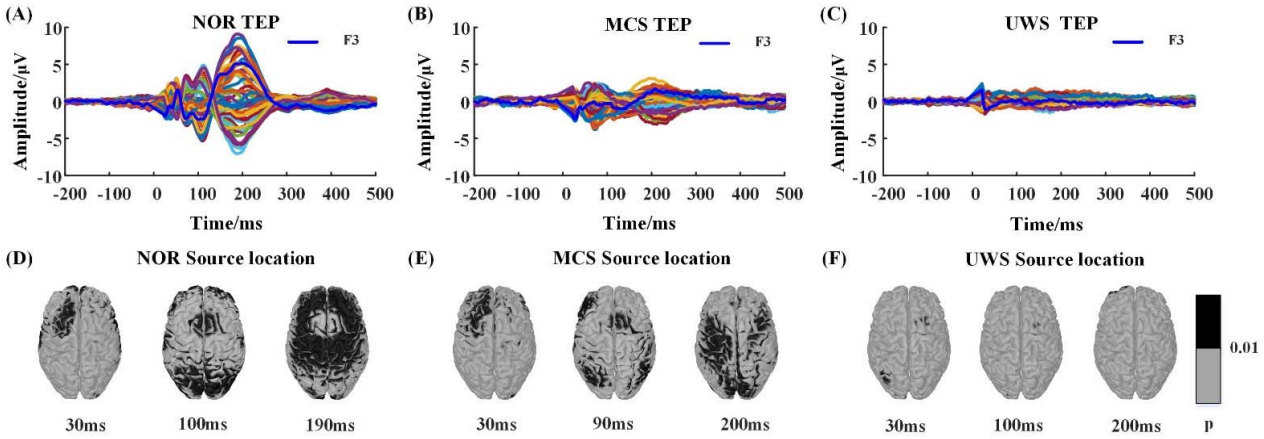

Fig. 2. TMS-evoked activity of NOR, MCS and UWS groups. (A-C) TEPs. (D-F) Maps of significant excitability at brain source level. 0 time is stimulation time. NOR: normal healthy adults, MCS: minimally consciousness state, UWS: unresponsive wakefulness syndrome.

series of components, such as P30, P60, N100 and P180. Analysis of TMS-evoked significant activity at brain source level shows TMS triggered complex activation of large-scale cortical regions. MCS shows smaller TEP amplitude, such as P30 and N100. MCS shows significant TMS-evoked excitability at source level from the stimulated site (frontal region) to distant sources (parietal and occipital regions) lasting to about 200ms. The UWS patient has no responses to TMS in according to the results of TEP components and excitability of brain source.

TEP time-space complexity of single NOR, MCS and UWS are shown in Figure 3. The TEP of NOR not only shows more spatial principal components (PC), but also has large amplitude and high temporal change rate. The number of independent spatial components of MCS is the same as NOR, but the amplitude of spatial principal components is smaller than that of NOR. The number and amplitude of spatial components of UWS is the smallest.

C. Group Results of PCIst With Different Parameters

PCIst shows significant differences with three parameters (*frequency*×*time*×*group*: F = 9.8, p < 0.001, df = 7667, Cohen's d = 0.06; *frequency*: F = 2092.7, p < 0.001, df = 7667, Cohen's d = 0.58; *time*: F = 1730, p < 0.001, df = 7667, Cohen's d = 0.53). But PCIst shows no significant differences with other three parameters (*frequency*×*sampling*×*group*: F = 0.01, p = 1, df = 3833, Cohen's d = 0; *sampling*: F = 0.01, p = 0.99, df = 3833, Cohen's d = 0).

1) Time: Time and group show a significant interaction effect (F=51.02, p<0.001, df = 7667, Cohen's d = 0.06). Figure 4 (A) shows the group difference of PCIst values between NOR and MCS, between MCS and UWS. When the data length of TEP is more than 200ms, PCIst shows significant differences between NOR and MCS, between MCS and UWS. There are no significant differences of PCIst values in the 21-100ms between MCS and UWS.

2) Sampling Rate: Sampling and group show no significant interaction effect (F=0.01, p=1, df = 3833, Cohen's d = 0). NOR and MCS, MCS and UWS show significant differences of PCIst values at the sampling rates, 1000Hz, 500Hz and 250Hz (Figure 5 (A)).

3) Frequency Band: Frequency and group show a significant interaction effect (F=99.07, p<0.001, df = 7667, Cohen's d = 0.12). Figure 5 (B) shows that PCIst values of NOR in 5 frequency bands are larger than MCS. PCIst values of MCS in 1-4Hz, 5-8Hz, 9-12Hz and 1-45Hz are significantly larger than UWS group.

D. Group Results of PCIst With Different Outcomes

We obtained the CRS-R results of 114 patients after one year and divided them into 2 groups, good outcome group (10.20±2.68) and poor outcome group (6.32±2.04). We compared PCIst values of different outcome groups. PCIst

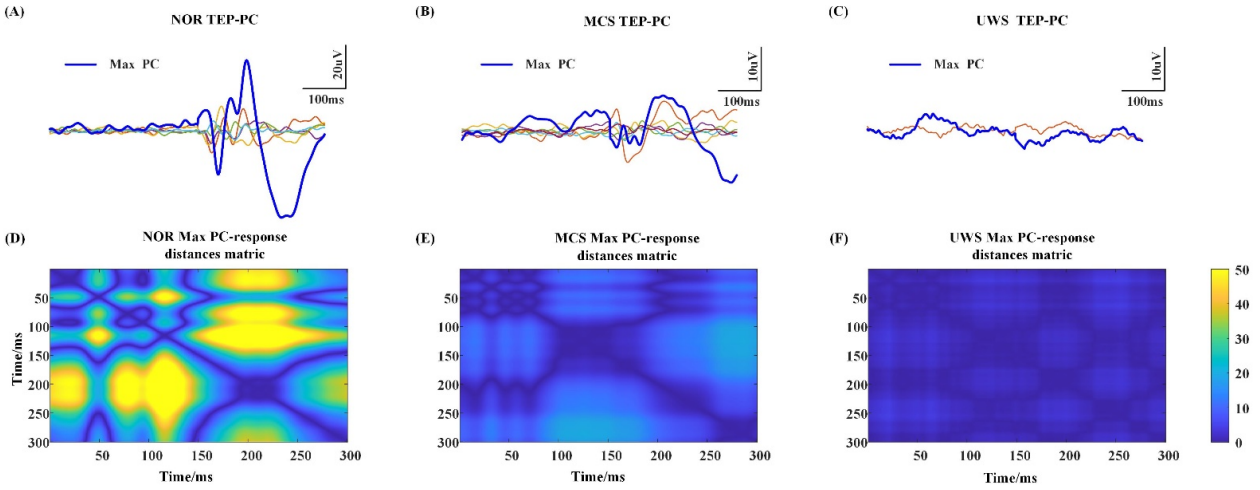

Fig. 3. TEP time-space complexity of NOR, MCS and UWS. (A-C) Spatial principal components (PC) of TEP after singular value decomposition and translation. (D-F) Distance matrices from recurrent analysis of the maximum principal component (Max PC).

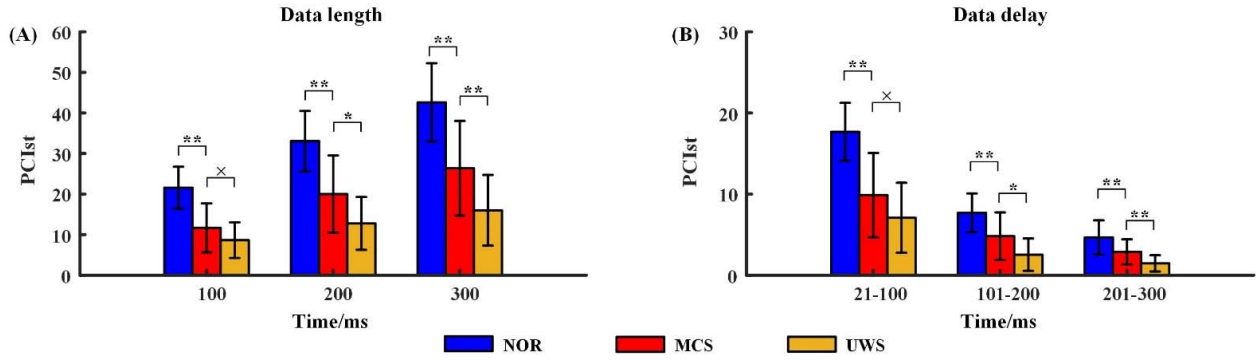

Fig. 4. PCIst with different data length and data delay settings. (A) Different data length of TEP response. (B) Different data delay of TEP response. Note: ×means p>0.05, *means p<0.05, **means p<0.005 followed by post hoc FDR corrected t-test. The bars represent the mean and error bars represent the standard deviation.

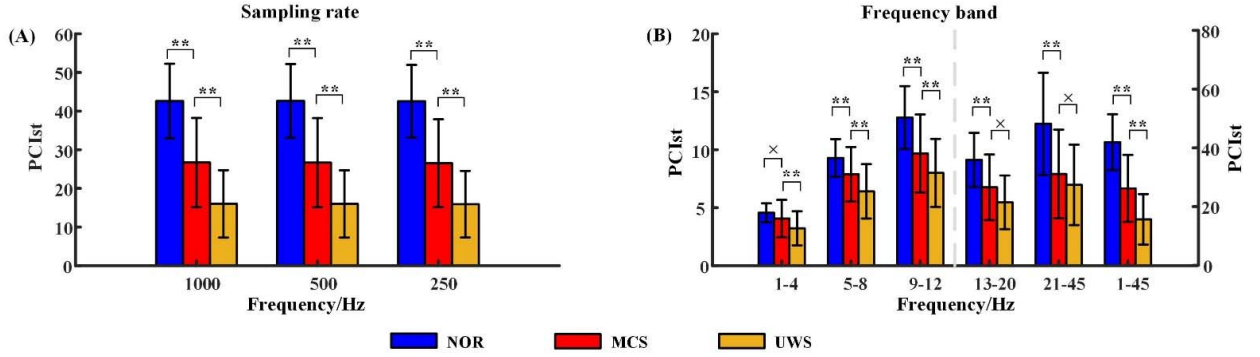

Fig. 5. PCIst wtih different sampling rate and frequency band settings. (A) Different sampling rates. (B) Different frequency bands. Left ordinate is for 1-4Hz, 5-8Hz and 9-12Hz, while right ordinate is for 13-20Hz, 21-45Hz and 1-45Hz. Note: ×means p>0.05, *means p<0.05, **means p<0.005 followed by post hoc FDR corrected t-test. The bars represent the mean and error bars represent the standard deviation.

values in five bands (1-4Hz, 5-8Hz, 9-12Hz, 13-20Hz and 1-45Hz) show significant differences between two groups (Figure 6 (A)). In addition, the proportion of MCS in the group with good outcome is high (31/54, 57.4%), while the proportion of UWS in the group with poor outcome is high (51/60, 85%).

E. Correlations

Baseline CRS-R shows significant correlation with PCI-lz ($r = 0.63$; $p<0.001$) and PCIst values in 1-4Hz, 5-8Hz, 9-12Hz and 1-45Hz (0.45, 0.48, 0.69, 0.61; $p<0.001$). CRS-R of patients after one year presents significant correlation with PCI-lz ($r= 0.59$; $p<0.001$) and PCIst in 1-4Hz, 5-8Hz, 9-12Hz and 1-45Hz (0.47, 0.43, 0.75, 0.57; $p<0.001$). PCIst in 9-12Hz shows the highest correlation with CRS-R after one year (Figure 6 (B)). PCIst in 13-20Hz and 21-45Hz show no significant correlation with CRS-R.

F. Results of Diagnostic and Prognostic Model

PCI-lz and PCIst in 9-12Hz and 1-45Hz are good at diagnosis (UWS versus MCS) and prognosis (good outcome versus poor outcome), and show top three correlation with consciousness level. We use above quantitative indexes of

TABLE II
PERFORMANCE OF EEG METRIC IN DIAGNOSIS AND PROGNOSIS OF DOC PATIENTS (MEAN ± SD)

	EEG indexes	SEN	SPE	F1 score	AUC	ACC
Diagnosis	PCIst(9-12Hz)	**0.839±0.006**	**0.799±0.013**	**0.849±0.008**	**0.893±0.003**	**0.822±0.008**
	PCIst(1-45Hz)	0.735±0.004	0.763±0.008	0.798±0.004	0.811±0.002	0.744±0.005
	PCI-lz	0.783±0.004	0.709±0.008	0.788±0.005	0.816±0.004	0.752±0.005
Prognosis	PCIst(9-12Hz)	**0.892±0.005**	**0.793±0.01**	**0.887±0.005**	**0.908±0.006**	**0.856±0.006**
	PCIst(1-45Hz)	0.775±0.003	0.683±0.01	0.802±0.004	0.811±0.004	0.748±0.005
	PCI-lz	0.691±0.022	0.527±0.04	0.757±0.008	0.624±0.041	0.655±0.018

Note: bold values mean best performance of diagnosis and prognosis.

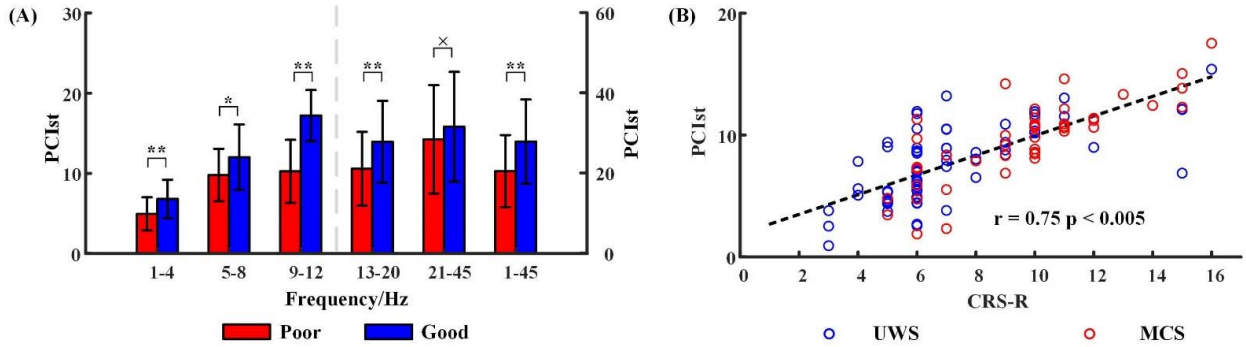

Fig. 6. PCIst of different outcome groups. (A) Differences of PCIst between two outcomes. (B) Correlation between PCIst in 9-12Hz and CRS-R after one year. Left ordinate of (A) is for PCIst in 1-4, 5-8 and 9-12Hz, while right ordinate of (A) is for PCIst in 13-20, 21-45 and 1-45Hz. Note: ×means p>0.05, *means p<0.05, **means p<0.005 followed by post hoc FDR corrected t-test. The bars represent the mean and error bars represent the standard deviation.

TMS-EEG to train SVM classification and SVM regression models for diagnosis and prognosis of DOC.

1) Confusion Matrix: Figure 7 and 8 plots the confusion matrix generated by the SVM after cross-validation. PCIst in 9-12Hz diagnoses UWS and MCS patients with 87% and 78% accuracy; Accuracy of diagnosis by PCIst in 1-45Hz is 87% and 58%; PCI-lz show accuracy of diagnosis with 80% and 70%. PCIst in 9-12Hz predicts poor and good outcome with 89% and 80% accuracy; Accuracy of prediction by PCIst in 1-45Hz is 85% and 56%; PCI-lz show accuracy of prediction with 82% on poor outcome, while has lower accuracy on good outcome (39%).

2) Performance: Figure 9 and Table II shows ROC curves and performance index (sensitivity, specificity, F1 score, AUC and ACC) of the SVM classification and regression models based on quantitative indexes of TMS-EEG. PCIst in 9-12Hz shows the highest cross-validation performance on classification between MCS and UWS. PCIst in 9-12Hz and PCI-lz show the almost equal performance of diagnosis.

Besides, PCIst in 9-12Hz presents the best performance on predicting the recovery outcome of DOC patients and PCIst in 1-45Hz band is the second place. PCI-lz shows the lowest performance among them as shown in Figure 9 (B) and Table II.

IV. DISCUSSION

PCIst is a fast and stable quantitative index of TMS-EEG, which can describe the temporal and spatial changes of cortical excitability. PCIst combines dimensionality reduction and recurrence quantification analysis to quantify time-space complexity of TMS-evoked brain activity. Singular value decomposition is performed to get the spatial principal component of TEP data. Recurrence quantification analysis is used to measure amplitude fluctuations of the principal components. PCIst is defined as sum of the maximized difference between response and baseline TEP data. Renzo et al reported PCIst can discriminate conscious from unconscious conditions on reduced EEG set-ups (19 and 8 electrodes). This study further investigates parameter selection of PCIst and uses PCIst for diagnosis and prognosis of DOC patients.

A. PCIst Shows Differences Among Different States of Consciousness

Like PCI-lz, PCIst shows significantly different values between different states of consciousness at the group level, but PCIst needs lower computational cost. Different states of consciousness show different results of TMS-EEG on TEP component number and amplitude. And PCIst decreases with the decrease of consciousness level. Similarly, Mario et al exported that patients showed more TMS-evoked cortical activity with the recovery of consciousness [11]. In addition, TMS-EEG study of sleep and anesthesia further confirmed that TEP could reliably monitor changes of consciousness in physiological and pharmacological conditions [24], [25]. Therefore, TEP is an EEG marker of cortical activation [39]. Cortical activation is the basis of higher cognitive functions, such as working memory and consciousness. The generation of

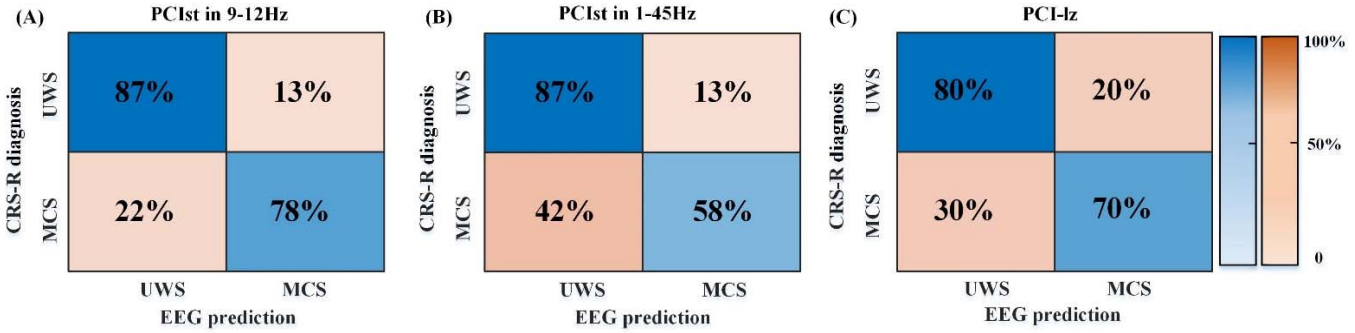

Fig. 7. Performance of diagnostic model based on EEG metric. Confusion matrix for (A) PCIst in 9-12Hz band. (B) PCIst values in 1-45Hz band. (C) PCI-lz in 1-45Hz band.

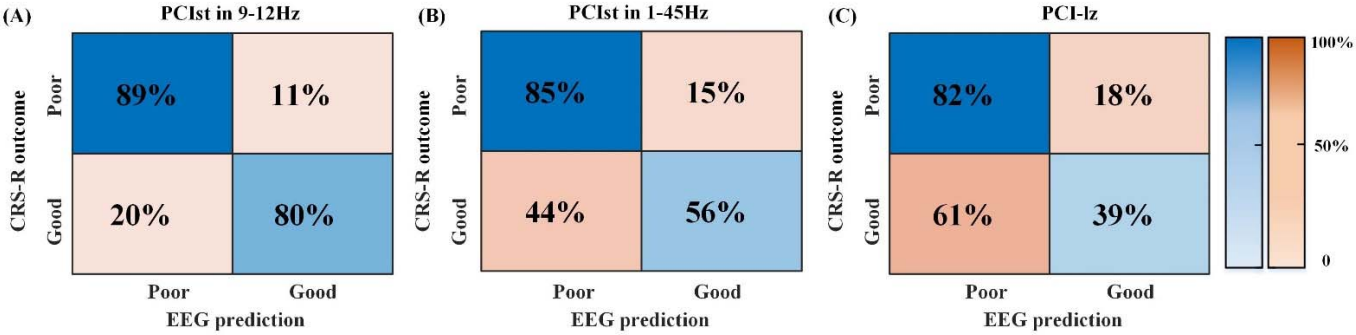

Fig. 8. Performance of prognostic model based on EEG metric. Confusion matrix for (A) PCIst in 9-12Hz band. (B) PCIst values in 1-45Hz band. (C) PCI-lz in 1-45Hz band.

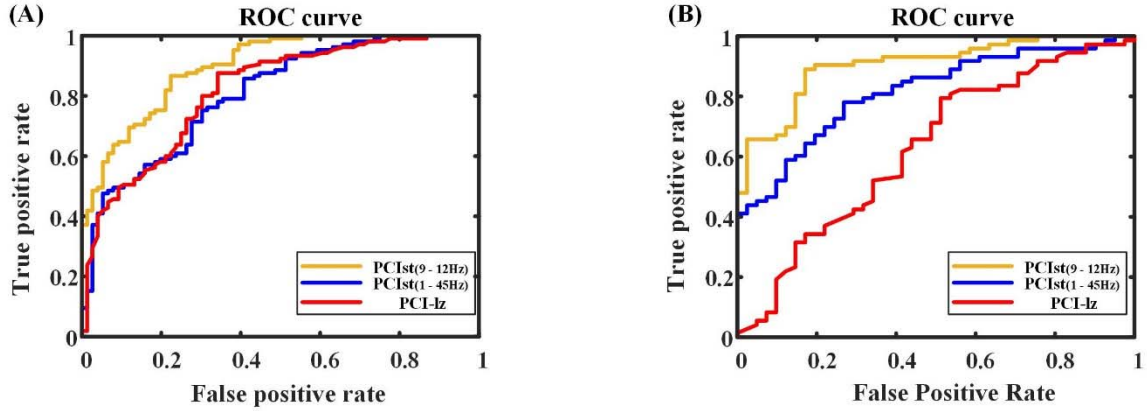

Fig. 9. ROC curves for diagnosis and prognosis models of DOC patients. (A) The ROC curves of PCIst values and PCI-lz for diagnosis. (B) The ROC curves of PCIst values and PCI-lz for prognosis. Yellow line is PCIst in 9-12Hz, blue line is PCIst in 1-45Hz and red line is PCI-lz.

consciousness involves the activation of multiple, specialized cortical areas. PCIst can quantify the temporal and spatial complexity of TEP from scalp EEG, and do so with lower computational cost. The results show that PCIst is a reliable and efficient quantitative index of consciousness level. The diagnostic models based on PCIst and PCI-lz show similar performance on diagnosis of DOC patients.

B. PCIst Values of Different States of Consciousness Are Affected by TEP Data Length

Our analysis shows that the optimal parameter for TEP data length is 300 ms after TMS, as this value maximizes TEP differences between different groups of DOC patients. Existing studies agree with the above result [11], [22], [35]. TEP generally lasts for 300 ms before returning to baseline level. The largest components of TEP related to primary motor cortex and dorsolateral prefrontal cortex are N280 and P180. TEP (0-300 ms) includes cortical activity in local and connected areas, while local cortical areas respond to TMS within 100ms [22]. UWS presents local and short-latency responses to TMS, while MCS shows more long-latency responses to TMS [11]. Our results provide evidence for differences of TEP in the time domain between NOR and DOC.

Based on the above results, we calculate PCIst for different TEP data delays after TMS. Results show that PCIst in 101-200ms and 201-300ms after TMS are different among NOR, MCS and UWS groups. The TEP data delay includes some special TEP components. The short-latency TEP component in 0-100 ms after TMS is related to the

excitability of stimulated cortex. In our results, PCIst values from 20-100 ms are significantly different between NOR and DOC, which concurs with forebrain dysfunction in DOC patients [40]. Similarly, neuroimaging studies have shown decreased frontal cortical activity in DOC patients [1], [40]. The long-latency TEP components in 101-200 ms and 201-300 ms, such as N100, P180 and N280, show activity of connected areas. The N100 peak over bilateral central sites likely represents GABA-mediated cortical inhibition, as N100 amplitude is affected by the process of intercortical inhibition [20], [23]. P180 and N280 show central and remote cortical activity. The long-latency TEP components are related to cortico-cortical interaction evoked by TMS. The decrease of TEP complexity in 101-300 ms of DOC patients may indicate widespread injury of cortico-cortical connectivity. Neuropathological studies have shown widespread structural and functional injury of cortico-cortical connectivity in DOC [11], [26], [41]. Our results not only show temporal and spatial differences in cortical responses for different states of consciousness, but also suggest impairment of cortical structural and functional connectivity in patients with DOC.

C. PCIst Values of Different States of Consciousness Are Not Affected by Low Sampling Rate But Affected by TEP Frequency Band

This study shows that PCIst values are still significantly different for different states of consciousness when TEP is down-sampled to 250 Hz. Data down-sampling is an important step in data preprocessing. Lower sampling rate, as long as meet the needs of data analysis, can reduce computational cost. The Nyquist theorem states that sampling rate must be at least twice the frequency of the low-pass filter. Various studies have sampled TMS-EEG data at 1000 Hz [18], 725 Hz [19] and 362.5 Hz [35]. We find that a sampling rate of 250 Hz is still suitable for TEP analysis.

In addition, our results show TEP differences among three groups in the frequency domain, especially in 5-8Hz and 9-12Hz bands. The model based on PCIst in 9-12Hz band has the best performance to diagnose MCS and UWS. TMS-EEG is often used to study local physiological mechanisms in terms of their natural frequency. Studies have found that TMS consistently evokes different dominant oscillations in different local cortices [19]. In addition, brain oscillation is related to cognitive activity. Theta band oscillatory activity involves memory, which requires information exchange between cortices [42], and cortical interaction is the foundation of conscious activity. Alpha band activity is an important marker of consciousness recovery [3], [16]. Research on consciousness have shown that dynamic EEG features in theta and alpha band are reliable EEG markers to distinguish different consciousness levels [13], [14]. Our study not only find differences of TMS-evoked cortical activity in time, but also show frequency differences of TEP.

D. PCIst Values in 9-12Hz Can Predict the Outcome of Consciousness Recovery

This study finds that PCIst values in 9-12Hz band could predict outcome of consciousness recovery in DOC patients. There are significant differences of PCIst values in 9-12Hz band between groups with different recovery results. In addition, baseline PCIst in 9-12Hz band is significantly related to the level of consciousness recovery (CRS-R) after one year. Furthermore, PCIst in 9-12Hz shows the best performance to predict different outcome groups. The prognostic model based on PCIst in 1-45Hz and PCI-lz present lower performance than PCIst in 9-12Hz. Previous studies have reported that EEG markers were useful for predicting the recovery of patients. DOC patients with re-establishment of resting EEG rhythmic activity, especially alpha rhythm, had better outcomes [43], [44]. The absence of early components of ERP predicted poor recovery, while cognitive components, such as N1, MMN and P3, were markers of good prognosis [16]. Most existing studies used TEP for consciousness diagnosis. This study, for the first time, uses TEP to predict DOC patients' consciousness recovery outcomes and broadens the clinical application of TMS-EEG. TEP components represent excitability of cortex and the interaction between cortices. Theoretical research, experimental data and clinical results suggest that effective cortical-cortical and cortical-subcortical connectivity are important factors in generating consciousness [40]. This study shows that the effective connectivity between brain regions is the marker of consciousness, and DOC patients who retained related brain functions have better recovery results.

V. Conclusion

In this study, we use PCIst to quantify the spatiotemporal complexity of TEP, investigate parameter selection of PCIst and explore the diagnostic and prognostic applicability of PCIst in DOC patients. We show that PCIst can quantify the level of consciousness. PCIst is a potential measure for the diagnosis and prognosis of DOC patients.

Acknowledgment

The authors are particularly thankful to the Seventh Medical Center of the Chinese PLA General Hospital for their cooperation and to Chen Xueling for recruiting participants and facilitating our study. They would also like to thank Dr. Li Zheng for his valuable suggestions on manuscript, and the editor and reviewers for their helpful comments to improve this manuscript.

References

[1] S. Laureys, A. M. Owen, and N. D. Schiff, "Brain function in coma, vegetative state, and related disorders," *Lancet Neurol.*, vol. 3, no. 9, pp. 537–546, 2004.

[2] J. T. Giacino *et al.*, "The minimally conscious state: Definition and diagnostic criteria," *Neurology*, vol. 58, no. 3, pp. 349–353, 2002.

[3] J. L. Bernat, "Chronic disorders of consciousness," *Lancet*, vol. 367, no. 9517, pp. 1181–1192, Apr. 2006.

[4] J. T. Giacino, J. J. Fins, S. Laureys, and N. D. Schiff, "Disorders of consciousness after acquired brain injury: The state of the science," *Nature Rev. Neurol.*, vol. 10, no. 2, pp. 99–114, Feb. 2014.

[5] J. T. Giacino, K. Kalmar, and J. Whyte, "The JFK Coma recovery scale-revised: Measurement characteristics and diagnostic utility," *Arch. Phys. Med. Rehabil.*, vol. 85, no. 12, pp. 2020–2029, 2004.

[6] C. Schnakers *et al.*, "Diagnostic accuracy of the vegetative and minimally conscious state: Clinical consensus versus standardized neurobehavioral assessment," *BMC Neurol.*, vol. 9, no. 1, p. 35, Dec. 2009.

[7] B. Zhang, G. Yan, Z. Yang, Y. Su, J. Wang, and T. Lei, "Brain functional networks based on resting-state EEG data for major depressive disorder analysis and classification," *IEEE Trans. Neural Syst. Rehabil. Eng.*, vol. 29, pp. 215–229, 2021.

[8] S. Panwar, S. D. Joshi, A. Gupta, and P. Agarwal, "Automated epilepsy diagnosis using EEG with test set evaluation," *IEEE Trans. Neural Syst. Rehabil. Eng.*, vol. 27, no. 6, pp. 1106–1116, Jun. 2019.

[9] Z. Jiang, F.-L. Chung, and S. Wang, "Recognition of multiclass epileptic EEG signals based on knowledge and label space inductive transfer," *IEEE Trans. Neural Syst. Rehabil. Eng.*, vol. 27, no. 4, pp. 630–642, Apr. 2019.

[10] O. Gosseries *et al.*, "Automated EEG entropy measurements in coma, vegetative state/unresponsive wakefulness syndrome and minimally conscious state," *Funct. Neurol.*, vol. 26, no. 1, pp. 25–30, 2011.

[11] M. Rosanova *et al.*, "Recovery of cortical effective connectivity and recovery of consciousness in vegetative patients," *Brain*, vol. 135, no. 4, pp. 1308–1320, Apr. 2012.

[12] A. Thul *et al.*, "EEG entropy measures indicate decrease of cortical information processing in disorders of consciousness," *Clin. Neurophysiol.*, vol. 127, no. 2, pp. 1419–1427, 2016.

[13] A. Piarulli, M. Bergamasco, A. Thibaut, V. Cologan, O. Gosseries, and S. Laureys, "EEG ultradian rhythmicity differences in disorders of consciousness during wakefulness," *J. Neurol.*, vol. 263, no. 9, pp. 1746–1760, 2016.

[14] D. A. Engemann *et al.*, "Robust EEG-based cross-site and cross-protocol classification of states of consciousness," *Brain*, vol. 141, no. 11, pp. 3179–3192, Nov. 2018.

[15] F. Wang *et al.*, "A brain–computer interface based on three-dimensional stereo stimuli for assisting clinical object recognition assessment in patients with disorders of consciousness," *IEEE Trans. Neural Syst. Rehabil. Eng.*, vol. 27, no. 3, pp. 507–513, Mar. 2019.

[16] R. Lehembre *et al.*, "Electrophysiological investigations of brain function in coma, vegetative and minimally conscious patients," *Arch. Italiennes Biologie*, vol. 150, nos. 2–3, pp. 122–139, 2012.

[17] M. Frantseva, J. Cui, F. Farzan, L. V. Chinta, J. L. P. Velazquez, and Z. Jeffrey, "Disrupted cortical conductivity in schizophrenia: TMS–EEG study," *Cerebral Cortex*, vol. 24, no. 1, pp. 211–221, 2014.

[18] N. C. Rogasch *et al.*, "Removing artefacts from TMS-EEG recordings using independent component analysis: Importance for assessing prefrontal and motor cortex network properties," *NeuroImage*, vol. 101, pp. 425–439, Nov. 2014.

[19] M. Rosanova, A. Casali, V. Bellina, F. Resta, M. Mariotti, and M. Massimini, "Natural frequencies of human corticothalamic circuits," *J. Neurosci.*, vol. 29, no. 24, pp. 7679–7685, 2009.

[20] F. Ferreri *et al.*, "Human brain connectivity during single and paired pulse transcranial magnetic stimulation," *NeuroImage*, vol. 54, no. 1, pp. 90–102, Jan. 2011.

[21] C. Bonato, C. Miniussi, and P. M. Rossini, "Transcranial magnetic stimulation and cortical evoked potentials: A TMS/EEG co-registration study," *Clin. Neurophysiol.*, vol. 117, no. 8, pp. 1699–1707, 2006.

[22] S. Komssi and S. Kähkönen, "The novelty value of the combined use of electroencephalography and transcranial magnetic stimulation for neuroscience research," *Brain Res. Rev.*, vol. 52, no. 1, pp. 183–192, 2006.

[23] N. C. Rogasch, Z. J. Daskalakis, and P. B. Fitzgerald, "Cortical inhibition of distinct mechanisms in the dorsolateral prefrontal cortex is related to working memory performance: A TMS–EEG study," *Cortex*, vol. 64, pp. 68–77, Mar. 2015.

[24] M. Massimini, F. Ferrarelli, R. Huber, S. K. Esser, H. Singh, and G. Tononi, "Breakdown of cortical effective connectivity during sleep," *Science*, vol. 309, no. 5744, pp. 2228–2232, Sep. 2005.

[25] F. Ferrarelli *et al.*, "Breakdown in cortical effective connectivity during midazolam-induced loss of consciousness," *Proc. Nat. Acad. Sci. USA*, vol. 107, no. 6, pp. 2681–2686, 2010.

[26] O. Gosseries, A. Thibaut, M. Boly, M. Rosanova, M. Massimini, and S. Laureys, "Assessing consciousness in coma and related states using transcranial magnetic stimulation combined with electroencephalography," *Annales Françaises D'Anesthésie Réanimation*, vol. 33, no. 2, pp. 65–71, Feb. 2014.

[27] P. C. Gordon *et al.*, "Modulation of cortical responses by transcranial direct current stimulation of dorsolateral prefrontal cortex: A resting-state EEG and TMS-EEG study," *Brain Stimulation*, vol. 11, no. 5, pp. 1024–1032, Sep. 2018.

[28] Y. Bai *et al.*, "Evaluating the effect of repetitive transcranial magnetic stimulation on disorders of consciousness by using TMS-EEG," *Frontiers Neurosci.*, vol. 10, p. 473, Oct. 2016.

[29] Y. Bai, X. Xia, J. Kang, Y. Yang, J. He, and X. Li, "TDCS modulates cortical excitability in patients with disorders of consciousness," *NeuroImage, Clin.*, vol. 15, pp. 702–709, Jan. 2017.

[30] A. N. Voineskos *et al.*, "The role of the corpus callosum in transcranial magnetic stimulation induced interhemispheric signal propagation," *Biol. Psychiatry*, vol. 68, no. 9, pp. 825–831, 2010.

[31] F. Ferrarelli *et al.*, "Reduced evoked gamma oscillations in the frontal cortex in schizophrenia patients: A TMS/EEG study," *Amer. J. Psychiatry*, vol. 165, no. 8, pp. 996–1005, Aug. 2008.

[32] F. Ferrarelli, R. E. Kaskie, B. Graziano, C. C. Reis, and A. G. Casali, "Abnormalities in the evoked frontal oscillatory activity of first-episode psychosis: A TMS/EEG study," *Schizophrenia Res.*, vol. 206, pp. 436–439, Apr. 2019.

[33] M. C. Pellicciari *et al.*, "Dynamic reorganization of TMS-evoked activity in subcortical stroke patients," *NeuroImage*, vol. 175, pp. 365–378, Jul. 2018.

[34] E. P. Casula *et al.*, "Subthalamic stimulation and levodopa modulate cortical reactivity in Parkinson's patients," *Parkinsonism Rel. Disorders*, vol. 34, pp. 31–37, Jan. 2017.

[35] A. G. Casali *et al.*, "A theoretically based index of consciousness independent of sensory processing and behavior," *Sci. Transl. Med.*, vol. 5, no. 198, Aug. 2013, Art. no. 198ra105.

[36] R. Comolatti *et al.*, "A fast and general method to empirically estimate the complexity of brain responses to transcranial and intracranial stimulations," *Brain Stimulation*, vol. 12, no. 5, pp. 1280–1289, Sep. 2019.

[37] B. M. Demaerschalk, S. Vegunta, B. B. Vargas, Q. Wu, D. D. Channer, and J. G. Hentz, "Reliability of real-time video smartphone for assessing national institutes of health stroke scale scores in acute stroke patients," *Stroke*, vol. 43, no. 12, pp. 3271–3277, 2012.

[38] N. C. Rogasch *et al.*, "Analysing concurrent transcranial magnetic stimulation and electroencephalographic data: A review and introduction to the open-source TESA software," *NeuroImage*, vol. 147, pp. 934–951, Feb. 2017.

[39] C. Miniussi and G. Thut, "Combining TMS and EEG offers new prospects in cognitive neuroscience," *Brain Topography*, vol. 22, no. 4, pp. 249–256, Jan. 2010.

[40] N. D. Schiff, "Recovery of consciousness after brain injury: A mesocircuit hypothesis," *Trends Neurosciences*, vol. 33, no. 1, pp. 1–9, Jan. 2010.

[41] S. Laureys, "The neural correlate of (un)awareness: Lessons from the vegetative state," *Trends Cogn. Sci.*, vol. 9, no. 12, pp. 556–559, 2005.

[42] N. Axmacher, M. M. Henseler, O. Jensen, I. Weinreich, C. E. Elger, and J. Fell, "Cross-frequency coupling supports multi-item working memory in the human hippocampus," *Proc. Nat. Acad. Sci. USA*, vol. 107, no. 7, pp. 3228–3233, 2010.

[43] M. Berkhoff, F. Donati, and C. Bassetti, "Postanoxic alpha (theta) coma: A reappraisal of its prognostic significance," *Clin. Neurophysiol.*, vol. 111, no. 2, pp. 297–304, 2000.

[44] P. L. Hansotia, "Persistent vegetative state: Review and report of electrodiagnostic studies in eight cases," *Arch. Neurol.*, vol. 42, no. 11, pp. 1048–1052, 1985.